Journal of Sound and Vibration 329 (2010) 2825–2842

Contents lists available at ScienceDirect

Journal of Sound and Vibration

journal homepage: www.elsevier.com/locate/jsvi

Excitation source of a side-branch shear layer

Hans R. Graf [a], Samir Ziada [b,*,1]

[a] Sulzer Innotec, Winterthur, Switzerland
[b] Laboratory for Fluid Mechanics and Acoustics, Ecole Centrale de Lyon, Ecully, France

ARTICLE INFO

Article history:
Received 8 June 2009
Received in revised form
8 January 2010
Accepted 28 January 2010
Handling Editor: P. Joseph
Available online 18 February 2010

ABSTRACT

The excitation source of flow-induced acoustic resonances in closed side-branches is characterized experimentally for circular pipes excited by turbulent flow in the main pipe. The shear layer at the branch junction is modeled by an unsteady complex source which is dependent on the Strouhal number and the acoustic particle velocity at the shear layer. The amplitude and phase of this source are determined experimentally and presented in the form of a dimensionless complex source term. This determined shear layer source term and the acoustic description of the piping system are then combined in a semi-empirical model to predict the frequency and pulsation amplitude of flow-excited acoustic resonance. The model results exemplify important experimental observations of flow excited side-branch resonances; including the occurrence of the lock-in phenomenon, the excitation of resonance by the single and double vortex modes of the shear layer, and nonlinear saturation at large pulsation amplitude due to vortex damping. The dependence of the pulsation amplitude on the Strouhal number, the static test pressure and on friction and radiation losses is also reproduced by the model. Finally, the effect of the acoustic particle velocity distribution at the branch junction on the shear layer source term is quantified.

1. Introduction

Flow past the opening of a closed side-branch or a deep cavity can excite strong acoustic depth-mode resonances. A good illustration of this effect is the tone that can be produced by blowing across the opening of a bottle. While the bottle-experiment is a popular demonstration of this fluid dynamic phenomenon, there are also important engineering applications. Flow induced side-branch oscillations can cause intense noise with discrete frequencies. The high amplitude of the acoustic pressure in the side-branch results in mechanical stresses in surrounding structures and can cause fatigue failure. The resonating side-branch also extracts energy from the flow, which can increase the fluid dynamic loss coefficient. Situations where these problems occur are commonly found in piping systems and in flows over deep cavities. A recent example of the damaging effects of this phenomenon is the acoustic fatigue damage of the steam dryer of a boiling water reactor in Quad Cities nuclear power plant. In this case, the pressure pulsations generated by acoustic resonance in the standpipes of safety relief valves propagated upstream in the main steam pipes and acoustically loaded the steam dryer [1–3].

Other case histories of flow-excited acoustic resonance in side-branches have been reported by Chen and Stürchler [4], Coffman and Bernstein [5], Bruggeman [6], among others. For example, Bruggeman [6] reported strong oscillations in

* Corresponding author.
E-mail addresses: hansrudolf.graf@sulzer.com (H.R. Graf), ziadas@mcmaster.ca (S. Ziada).
[1] Permanent address: McMaster University, Hamilton, Ontario, Canada.

0022-460X/$ - see front matter © 2010 Elsevier Ltd. All rights reserved.
doi:10.1016/j.jsv.2010.01.033

Nomenclature

A	cross-sectional area
D	diameter of main pipe=0.089 m
L	length of the side branch
M	Mach number
Str	Strouhal number=fd/U
U	mean flow velocity in main pipe (reference velocity)
V	dimensionless acoustic particle velocity (v/U)
Y	characteristic impedence $= \frac{\rho c}{A}\left\{1-\frac{\alpha}{k_o}+j\frac{\alpha}{k_o}\right\}$
Z	acoustic impedence $= \frac{\text{acoustic pressure}}{\text{acoustic volume velocity}}$
c	speed of sound
d	diameter of side branch (reference length)= 0.051 m
e	end correction
f	frequency of tone
k_0	$= \frac{2\pi f}{c}$
k	complex wavenumber (including attenuation) $=k_o+\alpha-j\alpha$
p	root-mean square of the acoustic pressure fluctuations
p_c	acoustic pressure fluctuations (rms) at the closed end of the side branch
p_s	static pressure of the fluid (absolute)
Δp	induced pressure difference across the shear layer (rms)
q	acoustic volume velocity=v A
s	source terms $\frac{\Delta p}{1/2(\rho U^2 V)}$
v	acoustic particle velocity (rms) at the branch opening (averaged over the cross-section)

Greek

α	acoustic absorption coefficient
ρ	density of the fluid

Subscripts

1, 2	referring to side branch 1 or 2
up, dn	referring to the upstream and downstream section of the flow pipe
j	referring of the junction

a pipeline installation for natural gas, where a manifold in a compressor station formed a system with multiple side branches. Acoustic pressure pulsations of up to 1.75 bar rms caused severe structural vibrations and made it necessary to avoid the operating conditions where resonance occurred. Jungowski et al. [7] investigated the effect of the diameter ratio on the Strouhal number and the oscillation amplitude of self-excited resonances, and Ziada and Bühlmann [8] demonstrated that multiple side-branches in close proximity are particularly liable to acoustic resonances because acoustically coupled branches can form a sub-system with negligible radiation losses. A good example of this case, which can often be found in the piping systems of power stations, chemical plants and natural gas compressor stations, is the so-called co-axial arrangement, where two closed side-branches of equal length are connected to the main pipe opposite to each other (Ziada and Bühlmann [8]). At the onset of acoustic resonance, the critical flow velocity in the main pipe can be predicted by means of the critical Strouhal number chart developed by Ziada and Shine [9]. This design chart can be used for industrial flow situations because it is developed from experiments on *cylindrical* side-branches connected to a main pipe conveying *high Reynolds number turbulent flow*. It also takes into account the effects of the side-branch arrangement (i.e. whether the side-branch is a single, a tandem or a co-axial branch), the diameter ratio between the side-branch and main pipe as well as the effect of approach flow distortions which may be caused, for example, by an upstream elbow.

While the excitation mechanism causing this phenomenon is fairly well understood based mainly on the analysis of 2-dimensional flow configurations, and the flow velocity at the onset of resonance can be predicted in most cases, it is still rather difficult to model the nonlinear interaction mechanism between the acoustic resonant field and the instability of the shear layer at the junction. This is particularly true for large amplitude pulsations in industrial applications where the flow at the junction of two cylindrical pipes is typically highly turbulent and three dimensional. A reliable model of this interaction mechanism is needed in order to be able to predict the nonlinear amplitude response of this resonance mechanism. This paper deals with the development of a dimensionless source term which describes the integral effect of the shear layer excitation due to its interaction with the sound field at the junction. The dimensionless frequency and amplitude of the sound field are considered to be the primary parameters which affect the shear layer excitation source term. Since the main aim of this work is to develop a model which can be used to predict the amplitude of pressure pulsations in industrial applications, the excitation source is determined from experiments on *cylindrical pipes conveying turbulent flow at high Reynolds numbers*.

2. Excitation mechanism

2.1. Feedback loop

Flow visualization studies, see e.g. [10,11], have revealed that during flow-excited acoustic resonance the shear layer across the opening of the side-branch rolls up into large scale vortex structures. As these vortices travel across the opening, they cause pressure fluctuations, which excite acoustic oscillations in the side-branch. The oscillations, in turn, initiate and

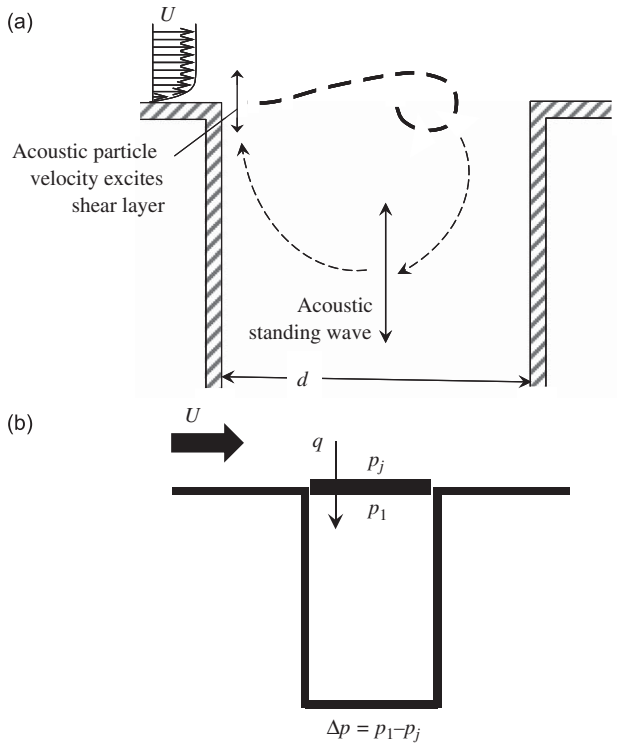

Fig. 1. (a) Feedback loop of the flow-excited side-branch resonance; (b) model of the shear layer excitation source during acoustic resonance in the side-branch. Δp is the pulsating pressure difference across the shear layer, spatially averaged over the cross-section.

synchronize periodic formation of new disturbances near the flow separation at the leading edge. This feedback loop is depicted in Fig. 1a. The overall gain of the feedback loop and the losses due to friction, heat conduction and radiation damping determine the amplitude of the acoustic oscillation. Since the acoustic standing wave provides the upstream feedback which excites the shear layer and sustains the resonance, Rockwell and Naudascher [12] categorized this type of self-excited resonance as "*fluid resonant*" oscillations. The behavior of the acoustic waves in the pipes is well understood and can readily be modeled; the excitation by the oscillating shear layer, however, is much more complex.

2.2. Theoretical models of the excitation mechanism

In the classical approach, the growth of small, wave-like disturbances in the shear layer is usually modeled with the linear stability theory [13]. The disturbances then give rise to an acoustic source which excites the oscillation, thus completing the feedback loop [12,14,15]. However, in the case of fluid resonances, the disturbance growth and the shear layer oscillation become highly nonlinear very rapidly. It is therefore more complex to describe the fluid resonant mechanism analytically.

Nelson et al. [16] used another approach to analyze the problem of flow-excited resonance in a Helmholtz resonator. They assumed the shear layer vorticity to be concentrated in a series of line vortices which are convected along the branch opening at a constant phase speed. The physics of the flow–acoustic interaction was then investigated in terms of momentum and energy exchanges occurring in the fluid itself. This alternative approach was explored because of the fact that the disturbances in the shear layer are large and can not be modeled appropriately by the linear or weakly nonlinear stability theories. To support this approach, Nelson et al. [17] carried out measurements of the flow field in the neck of a Helmholtz resonator excited to peak amplitude.

Since Howe [18,19] developed the integrand triple product concept which describes the sound power generated by vorticity transport in sound fields, many authors used this concept to model various aspects of the flow-excited acoustic resonance mechanism. Bruggeman et al. [20,21] modeled the flow in the junction of the side-branch with discrete vortices and identified the mechanism by which the moving vortices excite the acoustic oscillation. In this model, the acoustic power generated by the shear layer is proportional to the acoustic amplitude, i.e. the acoustic pressure induced by the shear layer oscillation is independent of the acoustic amplitude. The model also shows that the occurrence of resonance is dependent, to a large extent, on the timing between the acoustic oscillation and the propagation of the vortex along the

opening of the branch. This latter feature was also confirmed by means of numerical simulations, using the discrete vortex model, for other flow configurations and different acoustic mode patterns. For example, Stoneman et al. [22] explored the aeroacoustic sources for the case of flow over two tandem plates in a duct, in which vortex shedding from the plates excited the acoustic mode perpendicular to the flow. Hourigan et al. [23] investigated the excitation of longitudinal acoustic modes in a duct housing two baffles in close proximity. The importance of the timing between the acoustic oscillation and the vortex convection in the shear layer was also demonstrated experimentally by Graf and Durgin [24], using LDV measurements during the resonance of a deep cavity. In an extended vortex model based on Bruggeman's original idea, Graf [25] included the imaginary component of the excitation source. With this complex valued excitation source, the phase shift between shear layer excitation and acoustic oscillation can be taken into consideration. The above mentioned studies, however, were not intended to predict the amplitude of pulsation, but rather to better understand the excitation mechanism and predict the range of flow velocity over which the acoustic mode may be excited.

Subsequently, more elaborate models and numerical techniques were used to predict the pulsation amplitude as a function of the flow velocity. Kriesels et al. [11] used a two-dimensional potential flow model based on the vortex blob method to simulate the flow in the junction and calculate the acoustic power generated by the shear layer. Radavich et al. [26] simulated the two-dimensional flow at a *T*-junction by means of an implicit, noniterative method to solve the unsteady, turbulent and compressible Navier–Stokes equations. Although this simulation predicted correctly the extent of the lock-in velocity range and the resulting flow patterns exemplified the results of the flow visualization study reported by Ziada [10], the amplitude of pulsation was under-predicted by 50%. More recently, Dequand et al. [27] used Euler equations for two-dimensional compressible flow to perform numerical simulations at the junction of the co-axial branch case. This latter approach improved the prediction of the *maximum* pulsation amplitude to within 40% of the experimental results for the two-dimensional co-axial case. At other flow conditions, the prediction of the pulsation amplitude was less accurate. Slaton and Zeegers [28] suggested a different approach in which the total power generated by the aeroacoustic source can be determined by dissipating the acoustic power through known loss mechanisms. They demonstrated this approach by using a variable flow resistance and compliance placed at a pressure antinode to dissipate the acoustic power in a controlled manner.

Thus, despite much progress in the understanding and modeling of this phenomenon, the prediction of the pulsation amplitude is still problematic, especially for practical cases which involve fully developed turbulent flow in circular pipes.

2.3. Experimental approach

The foregoing discussion indicates that there is a need to develop a model which can be used in practical applications to predict not only the onset of resonance but also the pulsation amplitude as a function of flow and geometric parameters of the associated piping system. To that end, the nonlinear response of the shear layer instability, i.e. the excitation source, should be expressed as a function of the relevant parameters such as the frequency and the amplitude of the acoustic particle velocity at the branch opening. In this paper, an experimental technique is used to characterize this excitation source. The source amplitude and phase, with respect to the acoustic oscillation, are both required in order to be able to predict the resonant velocity range as well as the pulsation amplitude. Since the analytical description of the acoustic properties of the piping system poses no noticeable difficulties, this description can be combined with the above mentioned excitation source to develop a new semi-empirical model of self-excited resonance in piping systems.

The central concept of the source model developed in this paper is based on the following three hypotheses:

- The acoustic resonance is excited by a periodic pressure difference across the shear layer. This distributed pressure difference is induced by the moving vortex structures in the shear layer and its interaction with the geometrical singularities (Fig. 1a). However, for the proposed source model, only the *spatial average* of the pulsating pressure difference is considered as a "lumped" variable and represented by Δp (Fig. 1b). It should be emphasized that for the proposed source model, the excitation mechanism of the vortical flow structure does not need to be considered in detail, since this is accounted for in the experimentally determined parameters of the source term.
- The pressure difference Δp induced by the shear layer is only a function of "local" variables such as Strouhal number, acoustic particle velocity at the shear layer, velocity profile of the grazing flow, geometry of the pipe junction, etc. However, the pressure difference is *not* directly a function of the length of the side-branch or the acoustic impedance in the main pipe. As a first step, the parameters which are known to be most important are considered here; these being the Strouhal number and the amplitude of the acoustic particle velocity. The system nonlinearities are assumed to be confined to the growth and saturation of the shear layer disturbance and its interaction with the acoustic field. These nonlinearities are "local" characteristics of the junction region and, therefore, will be included in the measured source term of the shear layer excitation. The propagation of sound waves in the piping system as well as the associated friction, heat conduction and radiation losses will be dealt with by means of the linear theory of acoustics. This seems justifiable since the sound pressure level in the branch and main pipes is generally within the linear regime.

- The acoustic power generated by the unsteady flow is equal to the induced pressure difference Δp multiplied by the local acoustic volume velocity q (Fig. 1b). For steady-state oscillation, the power generated by the unsteady shear layer must be balanced by the visco-thermal dissipation and radiation losses of acoustic energy.

With these assumptions, the self-excited acoustic oscillation can be modeled as a harmonic oscillator excited by the vortex-induced pressure difference. Since the formation of the vortices in the shear layer is triggered by the acoustic oscillation in the junction, the pressure difference induced by the unsteady flow is periodic and synchronous to the acoustic oscillation. For the transfer of power from the flow to the acoustic oscillation, only the fundamental frequency component of the induced pressure difference is relevant. Higher harmonic components are expected to occur due to large amplitude nonlinear effects, however, their contribution to the excitation of the acoustic oscillation is usually small.

The fundamental frequency component of the pressure difference Δp is a complex value. The real part is in phase with the acoustic particle velocity and transfers active power between the flow and the acoustic oscillation. A positive real component of the pressure difference, for example, means the generation of acoustic energy which drives the acoustic resonance, whereas a negative real component leads to the absorption of acoustic energy which dampens the acoustic oscillation. The imaginary part is in phase with the acoustic acceleration of the fluid and is associated with the exchange of reactive power. A negative imaginary component of the pressure difference, for example, acts like an additional mass and tends to reduce the oscillation frequency.

3. Experimental technique

A series of experiments was designed to measure the pressure difference induced by the unsteady shear layer. First, the co-axial side-branches (Figs. 2a and 3a) were tested and the measured source term was validated against the measured pulsation amplitude for various geometry and flow conditions of the co-axial arrangement. Thereafter, two branches in the tandem arrangement (Figs. 2b and 3b) were tested to investigate the effect of the acoustic flux distribution at the branch opening on the complex source term of the shear layer excitation. In the latter case, the shear layer source term was measured for both the upstream and downstream branches. It should be emphasized that the source term presented in this paper is extracted from experiments on cylindrical pipes conveying a fully turbulent, three dimensional flow.

3.1. Test facility

The experiments were conducted in an open circuit piping system shown in Figs. 3 and 4. Two side-branches were attached to the flow pipe, first in the coaxial arrangement, Fig. 3a, and then in the tandem arrangement, Fig. 3b. The pipes were made of steel and the junctions of the side-branches with the main pipe had sharp edges. The inner diameter of the main pipe was D=89 mm and that of the branches was d=51 mm. To facilitate control over the acoustic oscillation, a loudspeaker was installed at the end of one side-branch. With this loudspeaker, an acoustic standing wave with specified amplitude and frequency could be excited in both side branches, thus overriding self-excitation.

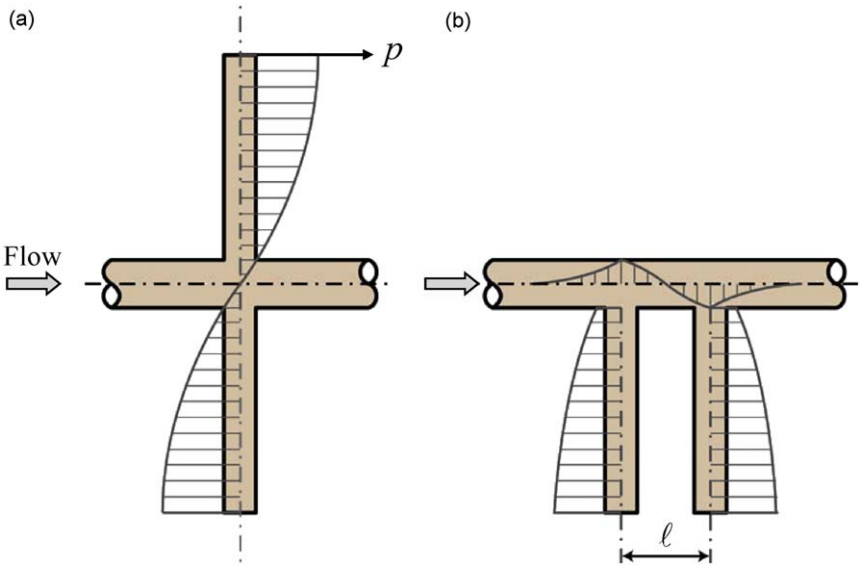

Fig. 2. Schematic presentation of two closed side-branches in (a) co-axial and (b) tandem arrangements showing the acoustic pressure distribution of the lowest resonance mode in both cases.

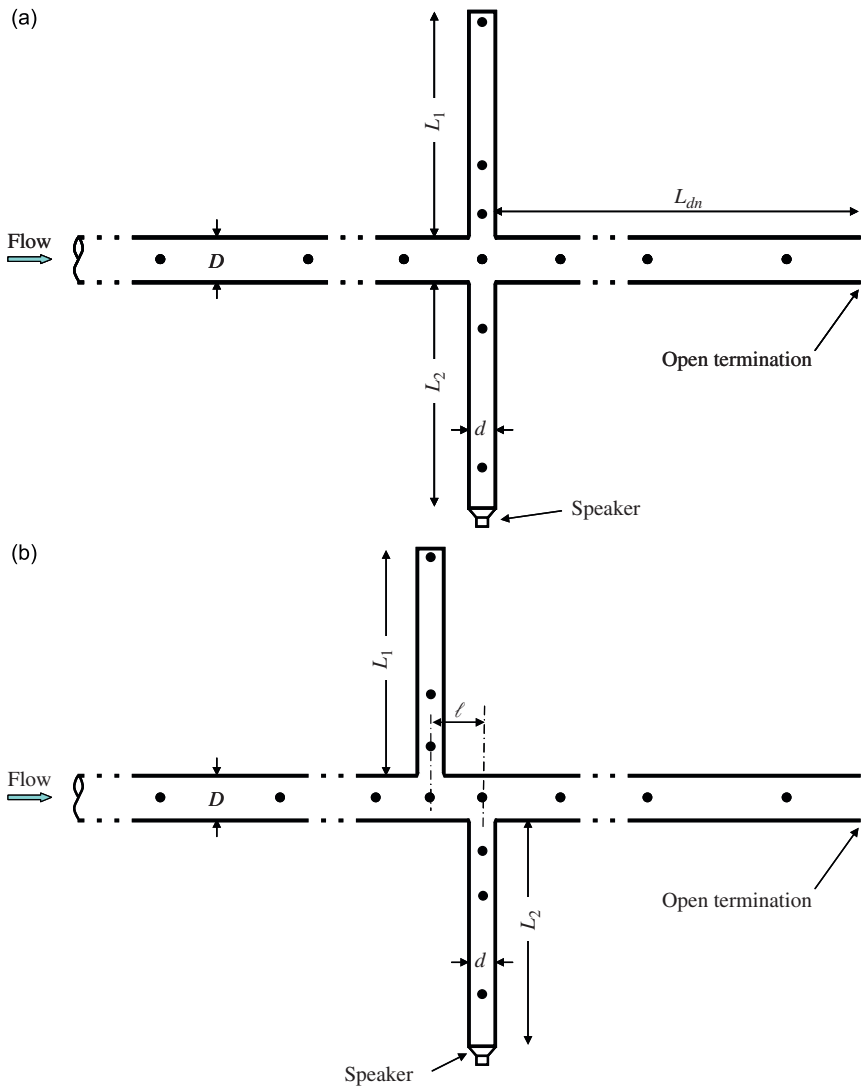

Fig. 3. Flow facility of (a) the co-axial branches and (b) the tandem branches. L_1=0.68 m, L_2=0.64 m, L_{dn}=2.1 m, D=89 mm, d=51 mm, ℓ=117 mm, microphone locations are indicated by ●.

As illustrated in Fig. 2, the length of both side-branches corresponded approximately to a quarter wavelength of the loudspeaker excitation frequency. The acoustic oscillation in both side-branches was therefore strongly coupled: acoustic flux coming out of one side-branch entered the second side-branch. The acoustic flux going into the flow pipe upstream and downstream of the side branches must be kept small in order to reduce attenuation through radiation of acoustic energy; otherwise the maximum rated power of the loudspeaker may not be sufficient to produce the intended amplitude of oscillation. Small acoustic flux into the flow pipe can be achieved by a high acoustic impedance of the main pipe at the junction. Downstream of the branches, the high impedance was accomplished by a pipe section of approximately $\frac{3}{4}$ wavelengths between the branches and the open end, where the flow was discharged into the atmosphere. This prevented the excitation of acoustic resonances in this pipe section. The acoustic reflections in the upstream pipe were weak; therefore, no special provisions were required.

The air needed to operate the flow model was taken from a pressurized air supply equipped with a moisture removal filter and therefore the test air was considered dry. The maximum capacity of the air supply was 0.5 kg/s and the flow rate was adjusted by means of a low-noise pressure regulator followed by an absorption silencer. The flow rate was measured by means of a standard metering orifice. The actual air temperature was recorded in order to determine the speed of sound. An elbow was located 33 pipe diameters upstream of the junction, and the silencer was positioned about 59 pipe diameters upstream of the elbow. The maximum Reynolds number in the main pipe during the tests was 5×10^5, but that at the onset of resonance was less than 2.6×10^5.

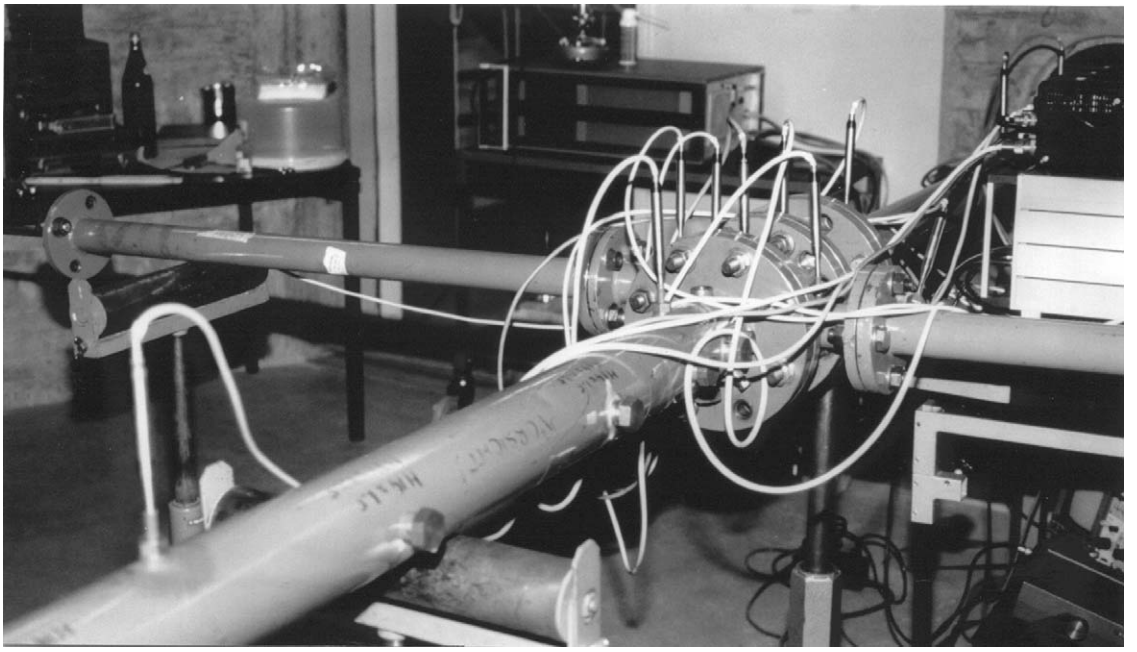

Fig. 4. Photograph of the experimental set-up of the tandem test case showing the microphone array.

In all experiments, the oscillation was forced with the loudspeaker at a constant frequency of 113 Hz, which is the resonance frequency of the side-branches. First, the flow in the main pipe was adjusted to obtain the desired Strouhal number. Thereafter, the volume of the loudspeaker was increased until the acoustic amplitude reached the appropriate level and the data acquisition was started. The forgoing procedure was repeated for different flow velocities, corresponding to the desired range of Strouhal number. During the tests of the tandem arrangement, Fig. 3b, the loudspeaker was attached to the downstream branch and the source terms of the upstream and downstream branches were evaluated at the same time. As illustrated in Fig. 3b, the tandem branches were attached to opposite sides of the main pipe to minimize the effect of the flow turbulence at the upstream branch junction on the shear layer source term determined for the downstream branch junction. The velocity profile of the flow in the main pipe was not measured, however, it was considered to be fully developed turbulent flow, similar to that encountered in industrial applications, because the Reynolds number used in the tests was high (of the order 10^5) and the pipe upstream of the branches was long (≈ 90 pipe diameters). In addition, the effect of changes in the boundary layer as the flow velocity was increased during the tests was not studied. As mentioned in Section 2.3, the parameters which are known to be most important are considered here as a first step; these being the Strouhal number and the amplitude of the acoustic particle velocity. The effect of other parameters, such as the boundary layer thickness of the approach flow will be considered in future studies.

3.2. Data acquisition

The pressure difference induced by the unsteady shear layer cannot be measured directly; instead it was calculated from the acoustic pressure which was measured with flush mounted 1/4″ microphones at 13 different positions in the piping system. A 16 channel FFT analyzer was used to process the microphone signals simultaneously.

The relative sensitivity and phase response of the microphones are critical for accurate results. In order to calibrate the microphones, they were mounted around a test-chamber shown in Fig. 5. The cavity in the center of the test block was driven by a loudspeaker and the relative amplitude and phase of the microphone signals were measured. The absolute sensitivity of one of the microphones was calibrated with a pistonphon. The measurements in the piping system were then corrected according to this calibration.

3.3. Data analysis

The acoustic waves in a section of pipe can be computed from the pressure signals measured by two microphones separated by an axial distance. The computational procedure is based on the theory by Munjal [29], describing plane acoustic waves in pipes. For sufficient accuracy, the effects of flow and attenuation are taken into account. At these low frequencies, the assumption of plane wave propagation is adequate and the higher order transverse (or cross) modes which are generated in the vicinity of the junction decay very rapidly after a short distance. For example, the first transverse mode

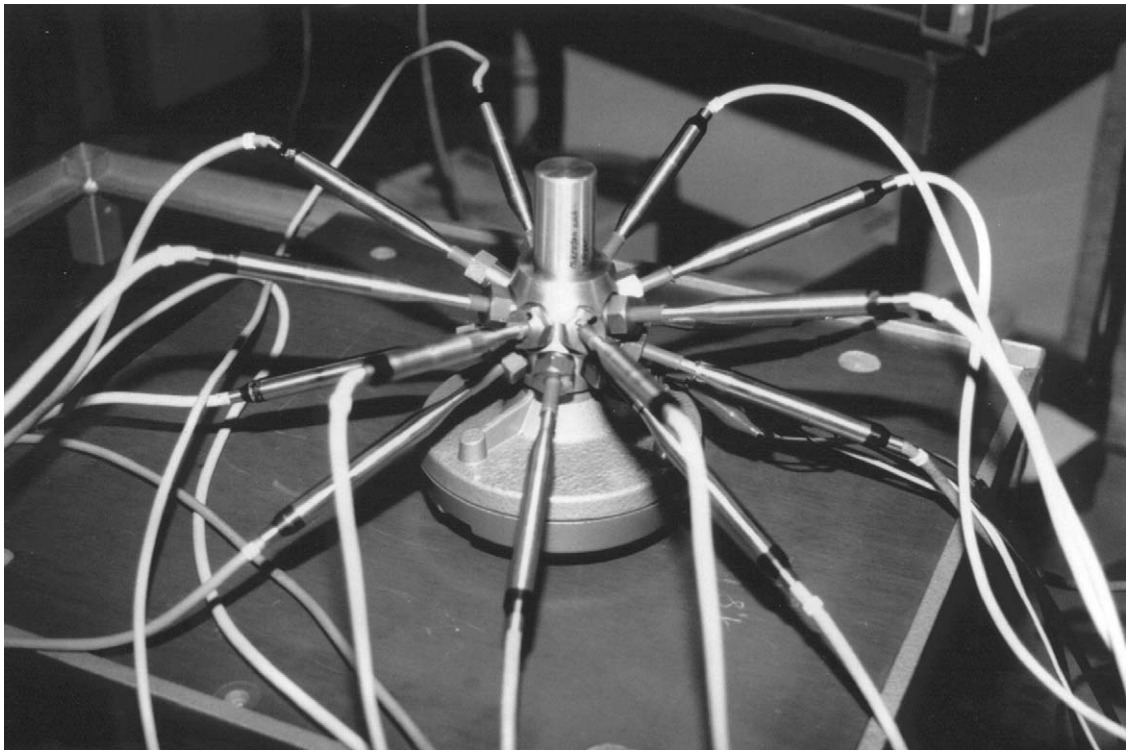

Fig. 5. Photograph of the test chamber used to calibrate the microphones.

decays proportional to $e^{-3.68x/D}$ or -32 dB/diameter; the second and higher transverse modes decay even steeper than the first. The closest microphone is 2.3 D upstream of the junction, where the first transverse mode is attenuated by 74 dB.

From the amplitude and phase of the microphone signals at the forced oscillation frequency (113 Hz), the acoustic waves in the different sections of the piping system were computed. In the flow pipe, the acoustic pressure was measured upstream and downstream of the branches at three positions; providing three pairs of pressure signals. The acoustic waves were computed from each microphone pair and then averaged in order to improve accuracy and reliability. The microphone in the center of the junction was only used for comparison.

After the acoustic waves in the piping system were determined, the acoustic pressure at the desired side-branch junction was extrapolated. The pressure on one side of the shear layer was computed from the waves in the flow pipe, while the pressure on the other side was determined based on the waves in the side branch, based on 2 or 3 microphone signals, respectively. The pressure difference Δp across the shear layer was then computed. For the computation of the pressure on the branch side of the shear layer, an end correction must be applied in order to compensate the additional mass in the region of the junction. With an end correction of $e=0.25D$, the imaginary part of the source term vanishes for $Str\rightarrow\infty$ (no flow). This corresponds to 87% of the branch radius and is very close to the theoretical value of 85% for a flanged end (Munjal [29]).

In the case of co-axial branches the extrapolated pressures from the upstream and the downstream measurements are supposed to be identical. Actually, these measurements yielded about the same acoustic pressure at the junction (difference usually few per cent) and the two values were averaged for further improved accuracy. The pressure measurements directly at the junction were less reliable, possibly due to the highly unsteady flow field in the junction.

3.4. Accuracy

The pressure difference Δp induced by the unsteady shear layer is rather small; it is on the order of 1% of the acoustic pressure at the closed end of the side-branches. The value of Δp is determined as the difference of two pressure values, which are both affected by several sources of inaccuracy. It is therefore difficult to calculate Δp accurately. Estimating the error is impractical, since it varies greatly with the actual parameters. In order to check the accuracy of the data, the resulting balance of acoustic flux and acoustic power at the junction were computed. For the case of co-axial branches, for example, the error in acoustic flux (flow toward junction minus flow away from junction) was quite small: less than 0.5% of the total acoustic flux at the junction. The difference between generated and dissipated power was usually about 1% of the total power generated by the shear layer. In few cases however, the error of the power balance was as high as 10%.

4. Results

The pressure difference across the shear layer was determined experimentally, covering Strouhal numbers from 0.25 to 1 and amplitudes of the acoustic particle velocity from 0.3% to approximately 50% of the flow velocity in the main pipe. The Strouhal number and the amplitude of the acoustic oscillation are considered to be the two most important parameters. In this section, the results of the case with co-axial branches are given.

The pressure difference induced by the unsteady shear layer is normalized by the dynamic pressure of the flow in the main pipe, $(1/2)\rho U^2$. In order to relate it to the acoustic properties of the piping system, this excitation term is divided by the dimensionless amplitude of the spatially averaged acoustic particle velocity at the branch opening, $V=v/U$. The resulting source term, s, then becomes a dimensionless acoustic impedance and has the form

$$s = \frac{\Delta p}{(1/2)\rho U^2 V} \tag{1}$$

Fig. 6 shows the dependence of the complex source term s on the Strouhal number and the oscillation amplitude. Each symbol indicates one value of s based on a steady-state measurement at the corresponding Strouhal number Str and amplitude V. The solid lines indicate the locus of s for some selected amplitude levels; the dashed lines are the locus curves of s for selected Strouhal numbers. Both, solid and dashed lines, are two-dimensional interpolations of measured points.

The Strouhal number, Str, has primarily an effect on the argument, i.e. the phase of s, and therefore it controls the phasing between the shear layer oscillation and the acoustic field, in accordance with the observation discussed in Section 2. On the other hand, the oscillation amplitude, V, influences mainly the modulus, or the absolute value of s. The solid lines with constant amplitude form a spiral around the origin of the complex s-plane.

As discussed earlier, acoustic power will be generated if the real part of the shear layer source is positive, which corresponds to the right hand side of Fig. 6. The left hand side therefore corresponds to the absorption of acoustic energy by the shear layer. The smallest amplitude case shown in Fig. 6 corresponds to an acoustic particle velocity of only 1% of the mean flow velocity. This small amplitude represents the source behavior at a low level of acoustic pulsation, i.e. near the beginning of the lock-in resonance range, where nonlinear effects related to shear layer saturation are still small. It is interesting to follow the spiral for this small amplitude, $V=0.01$, as the flow velocity is increased, which corresponds to a gradual decrease in the Strouhal number from unity. The real part of the source term becomes positive, i.e. acoustic excitation is possible, for two ranges of Strouhal number. First, from $Str \approx 0.92$ to 0.75, which corresponds to the formation of two vortices in the branch opening, and then from $Str \approx 0.53$ to 0.3, where a single vortex is formed at the branch junction. These ranges of Strouhal number are in good agreement with the experimental observations reported for a similar arrangement of cylindrical branches [8–10]. In those experiments, self-excited resonance occurred at the single vortex mode of the shear layer in the range $Str \approx 0.55$–0.28, and in the double vortex mode near $Str \approx 0.85$. The resonance was particularly strong near $Str \approx 0.42$. Fig. 6 shows that around this Strouhal number, the real part of s at larger amplitude

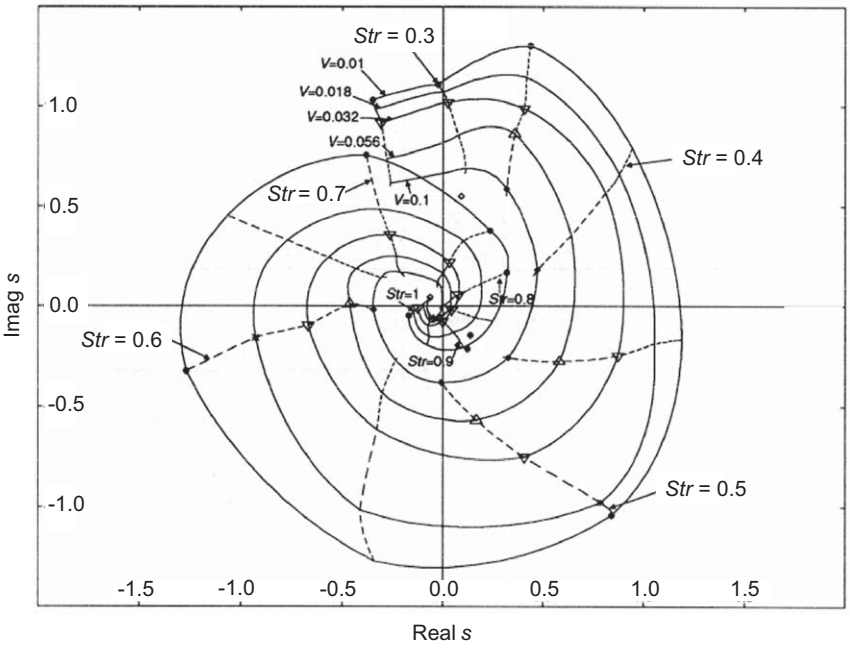

Fig. 6. Complex s-plane for small and moderate amplitudes of acoustic particle velocity. The parametric lines are "spirals" of constant particle velocity V, and "spokes" of constant Strouhal number Str. The symbols indicate measured data points.

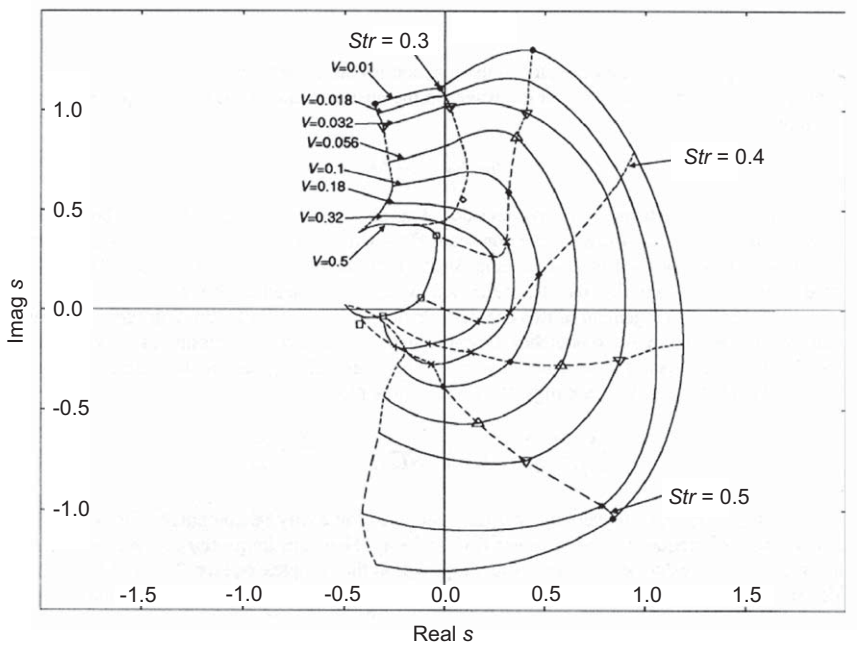

Fig. 7. Complex s-plane for the single vortex mode of the shear layer, including the whole range of tested amplitude from V=0.01 to 0.5.

is at its maximum and the imaginary part is close to zero. Another relevant experimental observation is the Strouhal number at the onset of acoustic resonance. Ziada and Shine [9] altered the visco-thermal losses in the branches by varying their lengths, while keeping them of equal length during each experiment, and found the Strouhal number at the onset of resonance to remain virtually constant near 0.55. Fig. 6 exemplifies this feature also as the real part of the source term at small amplitudes starts to become positive near this value of Strouhal number.

For Strouhal numbers slightly less than the maximum excitation level, which corresponds to the maximum real part of s, Fig. 6 shows the imaginary part of the source term to be positive. Therefore, the imaginary component of the pressure difference acts like an additional stiffness which increases the frequency of self-excited oscillation. This feature is also observed in the experiments. For Strouhal numbers slightly above the maximum excitation level, the imaginary component of s is negative; the induced pressure difference therefore acts like an additional mass, thus reducing the frequency.

For Strouhal numbers around 0.6, the real part of s is strongly negative. This indicates that the shear layer oscillation extracts energy from the acoustic oscillation. Shear layer oscillation at these Strouhal numbers could be induced only with very strong forcing by the loudspeaker.

As the oscillation amplitude increases, $|s|$ is reduced approximately proportional to $1/\sqrt{V}$. The induced pressure difference is therefore roughly proportional to $\sqrt{V}$. This is in contrast to the model suggested by Bruggeman et al. [21], where the driving pressure difference is independent of the amplitude.

Fig. 7 shows the parametric plot of s corresponding to the single vortex mode of the shear layer oscillation, including the curves for larger amplitudes up to V=0.5. As the oscillation amplitude increases, the center of the spiral connecting points of equal amplitude is shifted to the left. If the acoustic particle velocity is above $0.5U$, the real part of s remains negative for all Strouhal numbers, i.e. the shear layer becomes an acoustic sink and its oscillation extracts energy from the acoustic oscillation. This phenomenon, which results in nonlinear amplitude saturation of acoustic oscillations, is referred to in the literature as vortex damping [30,31] and has been predicted also by Bruggeman et al. [21].

5. Model validation

In this section, the measured source term of the co-axial branches and an analytical description of the piping system are combined in a semi-empirical model to predict the amplitude and frequency of the acoustic resonance. After describing the simulation procedure, the simulation results are compared with the experimental data of self-excited acoustic resonances to illustrate that the model is capable of predicting the pulsation amplitude and the effects of various system parameters, such as the flow velocity in the main pipe, the branch length, visco-thermal and radiation losses, as well as the effect of the static pressure inside the piping system.

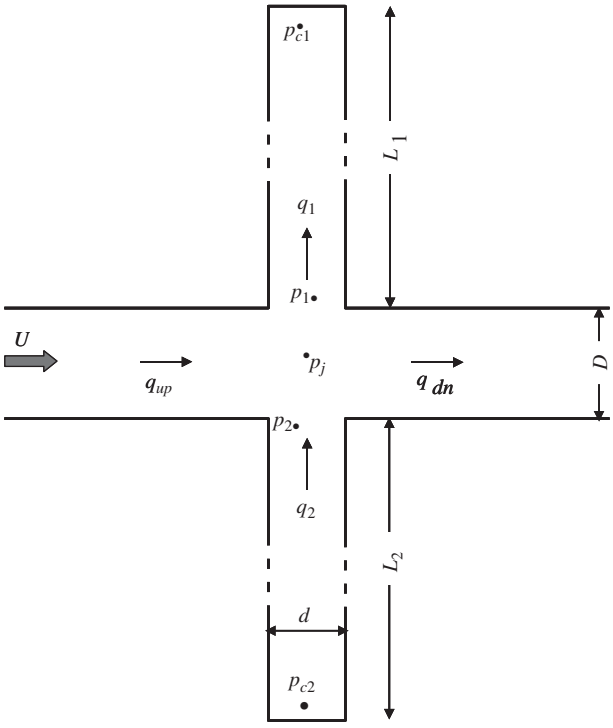

Fig. 8. Acoustic pressures and fluxes at the junction.

5.1. Simulation method

The methodology is first explained for the simple case of symmetrical co-axial branches and is then generalized for the case when the branches are not of equal length. As illustrated in Fig. 8, the acoustic properties of the piping system are determined by the acoustic impedances of the branches at the junctions. The impedance of side-branch 1 is given by

$$Z_1 = \frac{p_1}{q_1} = \frac{Y}{j \tan k(L_1 + e)} \tag{2}$$

The acoustic pressure on the branch side of the shear layer is then related to the acoustic flux by

$$p_1 = q_1 Z_1 \tag{3}$$

Similarly, the pressure in the flow pipe at the junction is determined by the acoustic waves in this pipe. This pressure must be identical for the waves in the upstream and in the downstream section of the flow pipe

$$p_j = q_{\mathrm{up}} Z_{\mathrm{up}} = q_{\mathrm{dn}} Z_{\mathrm{dn}} \tag{4}$$

The difference in acoustic pressure on both sides of the shear layer, $\Delta p_a = p_1 - p_j$, must be identical to the pressure difference Δp induced by the unsteady flow in the shear layer. A dimensionless acoustic impedance ΔZ is now obtained by normalizing Δp_a as described in Section 4 for Δp. The power generated by the source s and dissipated as described by ΔZ are balanced if $\Delta Z = s$.

In the symmetrical arrangement of two co-axial side-branches shown in Fig. 8, the acoustic wave can oscillate between the two side branches. Due to symmetry, the acoustic pressure in the junction is zero and there is no acoustic flux into the flow pipe. Therefore, ΔZ is given by the impedance of the side branch and is independent of the impedance in the flow pipe

$$\Delta Z = \frac{\Delta p_a}{1/2 \rho U^2} \frac{A_1 U}{q_1} = \frac{2}{M j \tan k(L_1 + e)} \left\{ 1 - \frac{\alpha}{k_o} + j \frac{\alpha}{k_o} \right\} \tag{5}$$

For a given geometry, flow velocity and frequency, ΔZ can easily be computed. Fig. 9 shows ΔZ as a function of frequency but for a constant flow velocity. Here the value of ΔZ is superimposed as solid squares on the complex s-plane and the frequency of ΔZ is indicated by the Strouhal number. When the length of the side-branch (including end correction) corresponds to a quarter wavelength, the imaginary part of ΔZ is zero. The real part of ΔZ describes the attenuation in the side branch due to friction losses and heat conduction. The condition $\Delta Z = s$ is satisfied at $Str = 0.45$. The corresponding oscillation amplitude $V = v/U = 0.075$ can be interpolated from the lines of constant amplitude in Fig. 9.

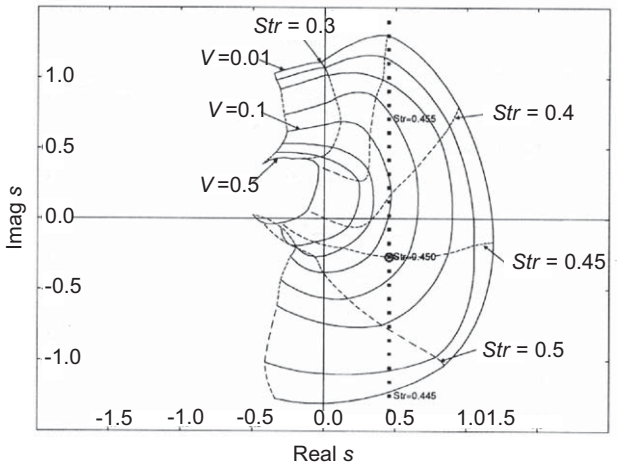

Fig. 9. Complex s-plane with superimposed ΔZ of a piping system with two co-axial side-branches. The symbols indicate ΔZ for different Strouhal numbers, i.e. different frequencies. At Str=0.45 the condition ΔZ=s is satisfied. The resulting amplitude of the self excited oscillation is V=0.075. Parameters for ΔZ are: U=12 m/s, c=342 m/s, L_1=L_2=0.801 m (including end correction), α=0.01 m^{-1}

In the general situation, the acoustic flux in the flow pipe is not zero. In this case, four variables are unknown: the Strouhal number, the amplitudes of the oscillation in both branches V_1 and V_2 and their relative phase. The graphical method illustrated in Fig. 9 for the symmetrical case is then not applicable. Instead, an iterative approach is used to solve the system of four nonlinear equations. This is accomplished with the Newton–Raphson method. Starting from a reasonable initial guess, the solution converges quickly after few iterations. Outside the lock-in range, where no valid solution exists because the resonance is not excited, the iteration diverges.

5.2. Comparison with experimental results

The amplitude of self-excited acoustic oscillation measured in experiments is compared to results obtained with the semi-empirical model. The experiments were performed in the flow facility described in Section 3.1, however, a valve was installed downstream of the side branches in order to facilitate measurements at higher static system pressure. The lengths of the side branches could be changed by movable pistons. Further details of the test loop and experimental results can be found in [8].

It should be mentioned here that the results of the semi-empirical model are compared to experimental data obtained from the same flow facility which was used to determine the characteristics of the excitation source. This leaves some questions open about the general applicability of the model to other piping systems. However, the range of the test conditions used to validate the model is much wider than the conditions used to determine the excitation source. For example, the experimental results used to validate the model correspond to several lengths of the side branches and to different values of the static system pressure. Moreover, the test results of asymmetric co-axial side-branches are also used for validation.

The pressure at the closed end of the side-branches, p_c, was measured and normalized by ρcU. Near resonance, this dimensionless parameter is approximately equivalent to V, which is an important parameter in our model. The value of $p_c/\rho cU$ is therefore preferable for the normalization than the dynamic head of the main flow, which is also used frequently in the literature.

5.2.1. Side branch modes and shear layer modes

Fig. 10 shows the predicted response of two coaxial branches of equal length (L_1=L_2=0.061 m). The amplitude and frequency of the self-excited oscillation are given as functions of the flow velocity in the main pipe. Oscillation occurs at three different frequencies corresponding to the side-branch modes $(1/4)\lambda$, $(3/4)\lambda$ and $(5/4)\lambda$. When the combination of flow velocity and one of the resonance frequencies results in a Strouhal number near 0.4, the single vortex mode of the shear layer generates a strong lock-in acoustic resonance. The shear layer double vortex mode excites the resonances at $Str \approx 0.85$, however, the oscillation is then much weaker.

As shown in Fig. 10, the simulation predicts the well known phenomenon of lock-in. As the flow velocity increases within the lock-in ranges, the oscillation frequency increases gradually from slightly below to slightly above the resonance frequency of the side-branches. This behavior agrees with the experimental findings in the literature [8,25,27]. This frequency shift is due to the imaginary part of the excitation source. At the beginning of the lock-in range (i.e. for Str slightly larger than 0.4), the imaginary part of the source term is negative and therefore it acts like an additional mass;

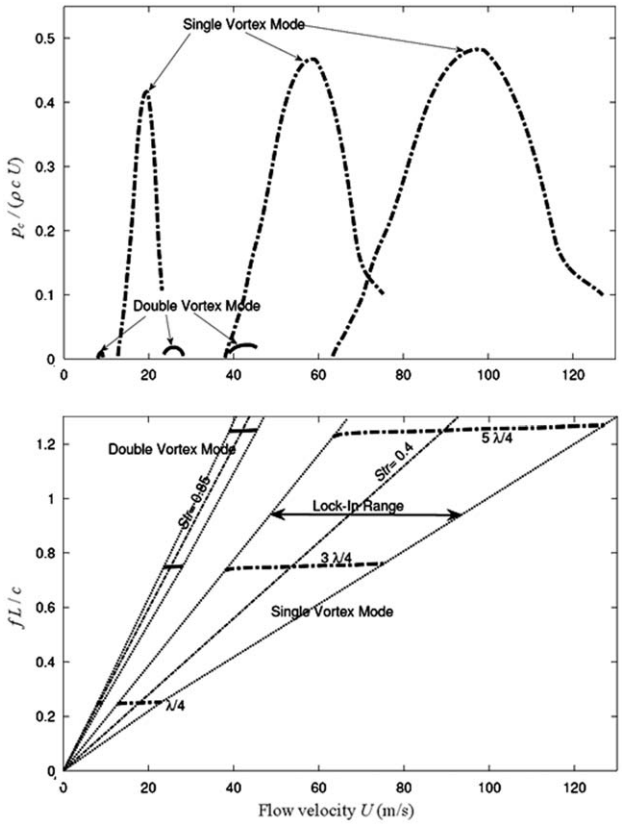

Fig. 10. Results of the semi-empirical model showing the amplitude and frequency of pressure pulsations at the closed end of the side-branch as functions of flow velocity in the main pipe. Symmetrical co-axial branches, c=342 m/s, L_1=L_2=0.61 m, p_s=4 bar.

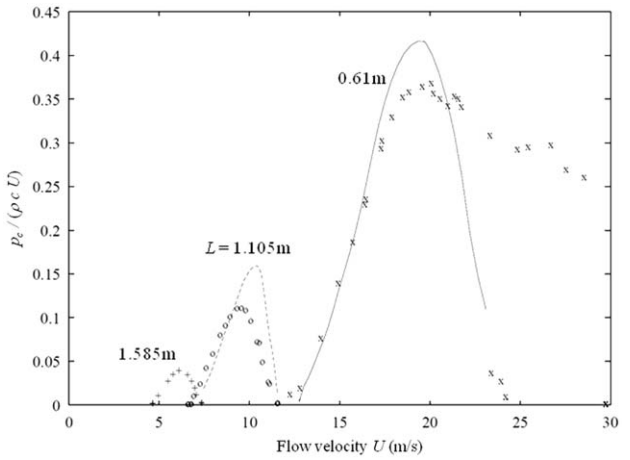

Fig. 11. Oscillation amplitude as a function of flow velocity for symmetrical co-axial side-branches with different lengths. The symbols indicate measured data for the first depth-mode resonance (λ/4 mode) and the lines are computed with the model. c=342 m/s, L_1=L_2=L, p_s=4 bar.

reducing the frequency of the self-excited resonance. For flow velocities near the end of the lock-in range, the imaginary part of the source term is positive, and the oscillation shifts to a higher frequency.

5.2.2. Effect of length of side-branch

The results presented in Fig. 11 were obtained with two coaxial side-branches of equal length. Here the effect of absorption by friction losses and heat conduction at the wall of the side branches is demonstrated. Due to the symmetry of the oscillation, acoustic losses in the main pipe (friction, thermal and radiation) are negligible. Since absorption increases

with the length of the side-branches, the amplitude is reduced as the branches are made longer. The oscillation amplitude and the lock-in range are seen to be well predicted by means of the developed semi-empirical model, also for the case with the largest pulsation amplitude which reaches $V \approx 0.37$. However, the hysteresis phenomenon for the shortest branches could not be reproduced. This phenomenon, which is commonly observed at large amplitude pulsations, might also be demonstrated by the model, when two (or more) points in the complex s-plane simultaneously match the load impedance ΔZ. However, an in depth analysis would be needed in order to investigate under which experimental conditions hysteresis can be observed and if the model, in fact, provides multiple solutions under similar conditions.

The importance of acoustic absorption in the side-branches is further delineated in Fig. 12. Here the length of the side branches was altered, but they were well tuned such that each of them constituted an odd number of quarter wavelengths (i.e. $(1/4)\lambda$, $(3/4)\lambda$ or $(5/4)\lambda$). In this way, the frequency in all cases remained approximately constant and a pressure node was always located at the junction; thereby minimizing the losses in the main pipe. Since the absorption is proportional to the total length of the side branches, the amplitude of oscillation is substantially reduced as the length of one branch is tripled (from $L_2=L_1=0.6$ m to $L_2=3L_1=1.8$ m) and then is reduced again when its length is increased to 5 times the length of the other branch ($L_2=5L_1=3$ m). Fig. 12 shows again that the oscillation amplitudes and the lock-in ranges are well predicted for all cases. It is interesting to note that for the case with $L_1=0.6$m and $L_2=3$ m and the case with $L_1=L_2=1.8$ m, the total length is the same in both cases and consequently the oscillation amplitudes are almost identical. As shown in Fig. 12, the model predicts this behavior also.

5.2.3. *Effect of radiation losses in the main pipe*

If two co-axial side-branches have slightly different lengths, the pressure node shifts from the center of the junction towards the longer side branch. Acoustic waves in the main pipe are then excited by the acoustic pressure in the junction. This leads to additional attenuation due to friction and radiation in the main pipe.

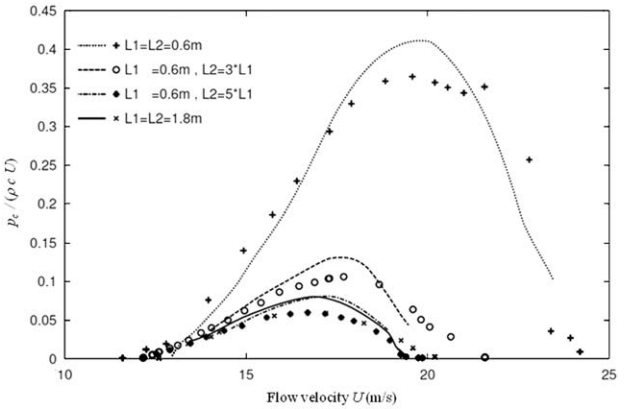

Fig. 12. Oscillation amplitude as a function of flow velocity for different depth modes of co-axial side-branches. The resonance frequency is 137 Hz in all four cases. The symbols indicate measured data and the lines are computed with the model. $c=342$m/s; $p_s=4$ bar; ⋯⋯, **+**, $L_1=L_2=0.6$ m; ——, **o**, $L_1=0.6$ m, $L_2=3L_1$; –·–·–·, ◆, $L_1=0.6$ m, $L_2=5L_1$; —, **x**, $L_1=L_2=1.8$ m.

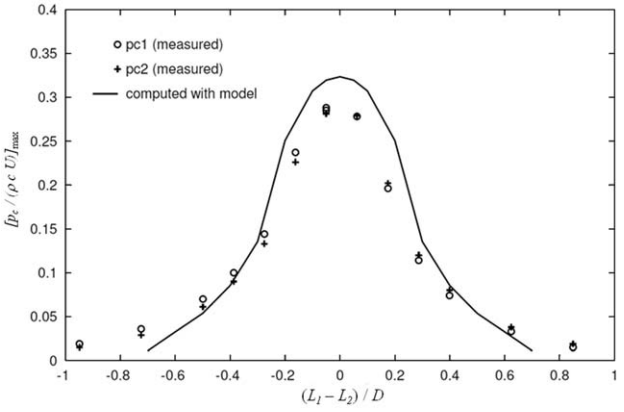

Fig. 13. Maximum amplitude of self-excited resonance in asymmetrical co-axial side-branches. The data show the effect of damping due to radiation losses in the main pipe. $c=342$ m/s; combined length $L_1+L_2=1.57$ m; $p_s=4$ bar; **o**, p_{c1}; **+**, p_{c2}; —, computed with model. Anechoic termination of the main pipe is assumed.

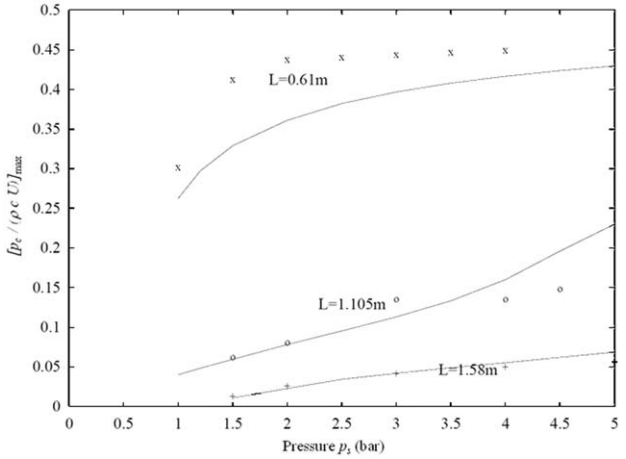

Fig. 14. Maximum oscillation amplitude as a function of static system pressure p_s for different lengths of symmetrical co-axial side-branches. The data corresponds to the first depth-mode resonance. The lines indicate results obtained with the semi-empirical model. $c=342$ m/s, $L_1=L_2=L$.

In Fig. 13, the length of one side-branch was increased in steps while the other side-branch was shortened accordingly by an equal length; thus keeping the resonance frequency constant while shifting the node towards the longer branch. The amplitude of the oscillation is significantly reduced when the lengths of the side-branches differ by as little as 30% of the main pipe diameter, D.

In the above asymmetric geometry used for demonstrating the effect of radiation losses, the oscillations in the two side branches are not identical. Therefore, the semi-empirical model was solved with the iterative Newton–Raphson procedure described in Section 5.1 in order to predict the frequency, the amplitudes of the oscillations in the two side branches and their relative phase. The model predictions in this more general case, with strong radiation in the main pipe, are seen to agree well with the experimental results.

5.2.4. Effect of system pressure

If the density of the fluid is increased, the Reynolds number increases as well. Sound absorption by friction forces therefore reduces in comparison with the dynamic forces generated by the excitation source. This leads to an increase in the oscillation amplitude for the same flow velocity. This effect has been observed experimentally by Jungowski et al. [7], Bruggeman [6] and Ziada and Bühlmann [8]. It can also be demonstrated by means of the developed semi-empirical model.

Fig. 14 shows comparisons between the model and the test results for three cases of co-axial side-branches as functions of the static test pressure. The increase in the oscillation amplitude is also predicted by the model. However, both the experimental and the model results show amplitude saturation near $p_c/\rho cU=0.45$, which is likely caused by the phenomenon of vortex damping [10,30,31].

6. Effect of particle velocity distribution

In the co-axial branch case, the branches are at opposite sides of the main pipe and therefore the particle velocity distribution at the branch opening can be considered to be fairly uniform. This would not be the case if a branch pipe is acoustically coupled with the upstream or the downstream section of the main pipe. In the former case, the acoustic flux, and the resulting particle velocity distribution, would be biased towards the upstream corner of the branch, which ought to increase sound absorption and reduce the source strength of the shear layer excitation. On the other hand, when the branch is coupled with the downstream section, the distribution of the acoustic particle velocity would be accentuated near the downstream corner of the branch, which ought to increase sound generation and the source strength. These effects are somewhat analogous to the effect of sharp or rounded edges at the upstream and downstream corners of the branch opening, as discussed in some detail by Bruggeman [6] and Ziada [32].

The above described effects of the particle velocity distribution on the shear layer excitation source can be investigated by means of the tandem branches test arrangement presented in Fig. 3b. In this case also, the system was excited at a constant frequency corresponding to the resonance frequency of the tandem branches and the measurement and data reduction procedures were similar to those used in the case of the co-axial branches. The measured source terms of the upstream and downstream tandem branches are shown in Fig. 15. The values of the Strouhal number and particle velocity amplitude for the various curves given in this figure are similar to those of the source term of the co-axial case which is shown in Fig. 7.

In Fig. 15a, corresponding to the downstream branch, the center of the "spirals", or the center of the innermost curve, is shifted to the left compared to that corresponding to the co-axial branch in Fig. 7. This agrees with the above supposition

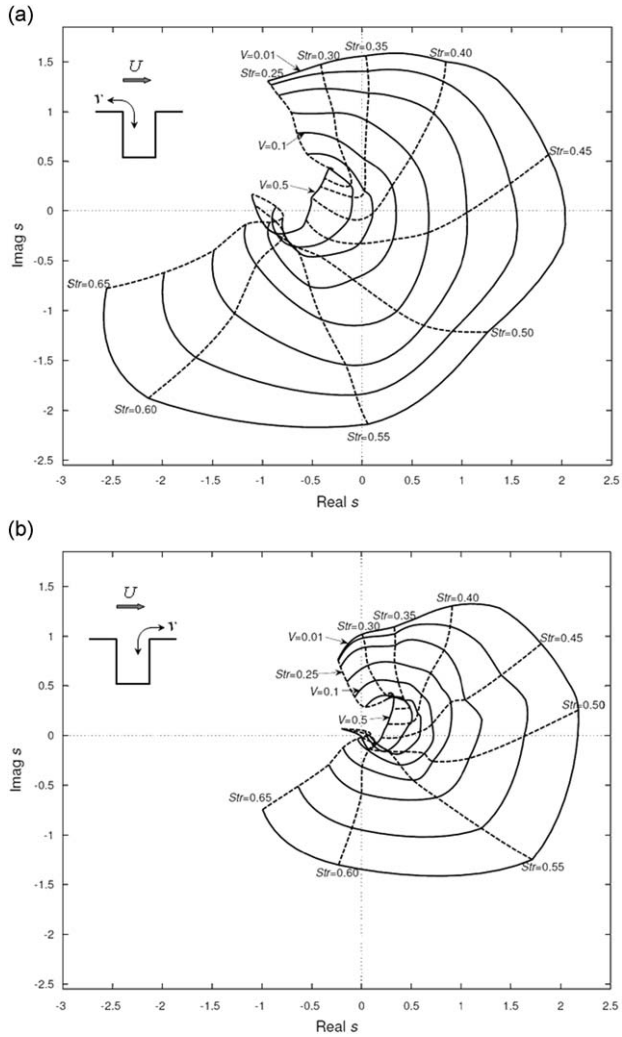

Fig. 15. Complex *s*-plane for the single vortex mode of the shear layer at the opening of tandem branches, including the whole range of tested amplitude from $V=0.01$ to 0.5. (a) Source term for the downstream branch; (b) for the upstream branch; v stands for the acoustic particle velocity.

that when the particle velocity is stronger near the upstream corner of the branch opening, more acoustic energy is absorbed. Thus, the innermost three curves corresponding to large amplitude pulsations, $V=0.18$, 0.32 and 0.5, are almost entirely in the left-hand side of the complex *s*-plane, indicating that the net effect of the shear layer at large amplitude pulsation is equivalent to a sink of aeroacoustic power. On the other hand, the center of the spirals for the upstream branch is seen in Fig. 15b to be shifted to the right compared to that of the co-axial branches (Fig. 7). In fact, the innermost three curves corresponding to large amplitude pulsations, $V=0.18$, 0.32 and 0.5, are entirely in the right-hand side of the complex *s*-plane, indicating that the shear layer is producing acoustic energy at these large amplitude pulsations. Further comparisons of the results for the upstream and downstream tandem branches, shown in Fig. 15a and b, illustrate clearly the effect of the particle velocity distribution on the complex source term of the shear layer, especially at large amplitude oscillations.

7. Summary and conclusions

Flow-induced acoustic resonance in closed side-branches is excited by an unsteady pressure difference across the shear layer. This unsteady pressure difference, which is induced by the generation and convection of vortex-like structures in the shear layer, is rather small. Nevertheless, it was successfully measured by means of an elaborate measuring system for a wide range of Strouhal numbers and oscillation amplitudes, which are considered to be the two most important parameters. The effects of the acoustic mode shape, i.e. the particle velocity distribution, at the junction region were also

investigated and characterized for the cases of co-axial and tandem closed side-branches. However, the effects of other parameters such as the corner geometry at the junction or the profile of the approaching boundary layer were not addressed.

The shear layer excitation source was measured for a fully turbulent pipe flow over the opening of a cylindrical side-branch. The amplitude and phase of the unsteady pressure difference across the shear layer, with respect to the particle velocity, are implemented into a complex source term which is presented in the form of a dimensionless impedance. The source term of the shear layer was then combined with a mathematical description of the acoustic properties of the piping system. This led to a new semi-empirical model of the flow-excited acoustic oscillation in closed side-branches.

The predictions of the developed excitation source model compare favorably with the experimental data. The oscillation amplitude, frequency and flow velocity at which they occur are predicted adequately for the cases of symmetric and asymmetric co-axial side-branches. The effects of acoustic attenuation by absorption in the side-branches and radiation into the main pipe are demonstrated. The model also explains features observed in experiments such as the phenomenon of vortex damping, the excitation of resonance by the single and the double vortex modes of the shear layer, as well as the slight increase in the resonance frequency as the system progresses into the lock-in velocity range.

The simulation results indicate that the acoustic properties of the piping system play an essential role and must be considered in the analysis of this self-excited phenomenon.

Acknowledgements

The work presented in this paper was part of a research program sponsored by the "Nationaler Energie Forschungs Fonds" of Switzerland and Sulzer Innotec Limited. The paper was prepared while the second author was a visiting professor at Ecole Centrale de Lyon.

References

[1] NRC, Failure of steam dryer cover plate after a recent power uprate. NRC Information Notice 2002-26, US Nuclear Regulatory Commission, Washington, DC, 2002.
[2] G. DeBoo, K. Ramsden, R. Gesior, B. Strub, Identification of Quad Cities main steam line acoustic sources and vibration reduction, *Proceedings of ASME PVP Conference*, San Antonio, Texas, Paper PVP2007-26658, 2007.
[3] S. Ziada, Flow-excited acoustic resonance in industry, Invited Paper, *Eighth International Conference on Flow Induced Vibrations*, Prague (2008). Also in Journal of Pressure Vessel Technology 132 (2010) 015001.
[4] Y.N. Chen, R. Stürchler, Flow-induced vibrations and noise in a pipe system with blind branches due to coupling of vortex shedding, *Internoise Zürich* 77 (1977) B189–B203.
[5] J.T. Coffman, M.D. Bernstein, Failure of safety valves due to flow-induced vibrations, *Journal of Pressure Vessel Technology* 102 (1980) 112–118.
[6] J.C. Bruggeman, Flow Induced Pulsations in Pipe Systems, PhD Dissertation, Technical University Eindhoven, Netherlands, 1987.
[7] W.M. Jungowski, K.K. Botros, W. Studzinski, Cylindrical side-branch as tone generator, *Journal of Sound and Vibration* 131 (1989) 265–285.
[8] S. Ziada, E.T. Bühlmann, Flow-excited resonances of two side-branches in close proximity, *Journal of Fluids and Structures* 6 (1992) 583–601.
[9] S. Ziada, S. Shine, Strouhal numbers of flow-excited acoustic resonance of closed side branches, *Journal of Fluids and Structures* 13 (1999) 127–142.
[10] S. Ziada, A flow visualisation study of flow–acoustic coupling at the mouth of a resonant side-branch, *Journal of Fluids and Structures* 8 (1994) 391–416.
[11] P.C. Kriesels, M.C.A.M. Peters, A. Hirschberg, A.P.J. Wijnands, A. Iafrati, G. Riccardi, R. Piva, J.C. Bruggeman, High amplitude vortex-induced pulsation in a gas transport system, *Journal of Sound and Vibration* 184 (1995) 343–368.
[12] D. Rockwell, E. Naudascher, Review self-sustained oscillations of flow past cavities, *Journal of Fluids Engineering* 100 (1978) 152–165.
[13] A. Michalke, On spatially growing disturbances in an inviscid shear layer, *Journal of Fluid Mechanics* 23 (1965) 521–544.
[14] S.A. Elder, Self-excited depth-mode resonance for a wall-mounted cavity in turbulent flow, *Journal of the Acoustical Society of America* 64 (1978) 77–890.
[15] M.S. Howe, The influence of mean shear on unsteady aperture flow with application to acoustical diffraction and self-sustained cavity oscillations, *Journal of Fluid Mechanics* 109 (1981) 125–146.
[16] P.A. Nelson, N.A. Halliwell, P.E. Doak, Fluid dynamics of a flow excited resonance, part II: flow acoustic interaction, *Journal of Sound and Vibration* 91 (1983) 375–402.
[17] P.A. Nelson, N.A. Halliwell, P.E. Doak, Fluid dynamics of a flow excited resonance, part I: experiment, *Journal of Sound and Vibration* 78 (1981) 15–33.
[18] M.S. Howe, The dissipation of sound at an edge, *Journal of Sound and Vibration* 70 (1980) 407–411.
[19] M.S. Howe, *Acoustics of Fluid-Structure Interactions*, Cambridge University Press, 1998.
[20] J.C. Bruggeman, A. Hirschberg, M.E.H. van Dongen, A.P.J. Wijnands, J. Gorter, Flow induced pulsations in gas transport systems: analysis of the influence of closed side branches, *Journal of Fluids Engineering* 111 (1989) 484–491.
[21] J.C. Bruggeman, A. Hirschberg, M.E.H. van Dongen, A.P.J. Wijnands, J. Gorter, Self-sustained aero-acoustic pulsations in gas transport systems: experimental study of the influence of closed side branches, *Journal of Sound and Vibration* 150 (1991) 371–393.
[22] S.A.T. Stoneman, K. Hourigan, A.N. Stokes, M.C. Welsh, Resonant sound caused by flow past two plates in tandem in a duct, *Journal of Fluid Mechanics* 192 (1988) 455–484.
[23] K. Hourigan, M.C. Welsh, M.C. Thompson, A.N. Stokes, Aerodynamic sources of acoustic resonance in a duct with baffles, *Journal of Fluids and Structures* 4 (1990) 345–370.
[24] H.R. Graf, W.W. Durgin, Measurement of the nonsteady flow field in the opening of a resonating cavity excited by grazing flow, *Journal of Fluids and Structures* 7 (1993) 387–400.
[25] H.R. Graf, Experimental and Computational Investigation of the Flow Excited Acoustic Resonance in a Deep Cavity, PhD Dissertation, Worcester Polytechnic Institute, Worcester MA, 1989.
[26] P.M. Radavich, A. Selamet, J.M. Novak, A computational approach for flow–acoustic coupling in closed side branches, *Journal of the Acoustical Society of America* 109 (2001) 1343–1353.
[27] S. Dequand, S.J. Hulshoff, A. Hirschberg, Self-sustained oscillations in a closed side branch system, *Journal of Sound and Vibration* 265 (2003) 359–386.
[28] W.V. Slaton, J.C.H. Zeegers, Acoustic power measurements of a damped aeroacoustically driven resonator, *Journal of the Acoustical Society of America* 118 (2005) 83–91.

[29] M.L. Munjal, *Acoustics of Ducts and Mufflers*, Wiley, New York, 1987.
[30] M.S. Howe, Contributions to the theory of aerodynamic sound, with application to excess jet noise and the theory of the flute, *Journal of Fluid Mechanics* 71 (1975) 625–673.
[31] D.W. Bechert, Sound absorption caused by vorticity shedding demonstrated with a jet flow, *American Institute of Aeronautics and Astronautics* (1979) Paper 79-0575.
[32] S. Ziada, *Flow-Excited Resonances of Piping Systems Containing Side-Branches: Excitation Source, Counter-Measures and Design Guidelines, Acoustic Pulsations in Rotating Machinery*, AECL, Toronto, 1993.